Magnetization Reversal Characteristics in NiFe Elliptical Ring Arrays

Liang-Juan Chang[1,2], Kuan-Yu Chen[1,3], Lu-Kui Lin[1], Yeong Der Yao[4], Pang Lin[2], and Shang Fan Lee[1,3]

[1]Institute of Physics, Academia Sinica, Taipei 11529, Taiwan
[2]Department of Materials Science and Engineering, National Chiao Tung University, Hsinchu 300, Taiwan
[3]Institute of Optoelectronic Sciences, National Taiwan Ocean University, Keelung, 202, Taiwan
[4]Institute of Applied Science and Engineering, Fu Jen University, Taipei 242, Taiwan

The magnetization reversal processes of single-layer nanoscale elliptical ring arrays are examined. The magnetic field was applied parallel or perpendicular to the long axis. The magnetization hysteresis loops showed a simultaneous-reversal single-step transition or two-step transition involving flux closure vortex states. For various aspect ratios and thicknesses, the transition between single-step and double-step magnetization reversals was measured to form phase diagrams. Simulations of the magnetization reversal behavior agreed with our results.

***Index Terms*—Magnetic films, magnetooptic Kerr effect.**

I. Introduction

THE application of nanotechnology to the information storage industry has resulted in a variety of products for high-density and low-cost data storage. Magnetic material nanotechnology applications that are readily commercially available include read head sensors [1] and magnetic random access memories [2]. Recently, arrays of magnetic nanorings have attracted intense investigations in both theoretical and experimental research for potential use in a wide range of magnetoelectronic devices [3]–[5]. The main interesting properties of ring-shaped nanomagnets are the formation of the two distinct states, a vortex state and an onion state, during magnetization reversal. The vortex state is a magnetic flux closure state without an energetic core at the center, which was found in a disk shape. The onion state has two domain walls present along the field direction on opposite sides of the ring [6], [7]. The vortex state has magnetic flux closure lines; thus the vortex state generates the smallest magnetostatic interaction between adjacent units. The phase diagram of magnetization switching behavior of a magnetic nano-ring as functions of geometrical parameters such as outer diameter, linewidth, and thickness was investigated in detail [3], [6]. More recently, the single-layer and multilayer elliptical rings have been introduced [8]–[11]. Besides similar characteristics of magnetization reversal to the ring shape, i.e., the vortex and the onion states, the elliptical rings have the advantage that the vortex stability is easily controlled by the shape anisotropy [11]. The magnetization switching behavior of pattern nanomagnets was influenced by the geometry of each unit and the interaction between the units [8], [12]–[14]. The magnetization reversal behavior and anisotropy energy effect of the elliptical rings has been investigated [12]. Jung *et al.* [8] reported the vortex chirality of elliptical rings as a function of external field orientation dependence on the energy change of the domain wall movements. Chang *et al.* [13] systematically studied different arrangements of the 2-D elliptical ring array on the magnetic dipole–dipole interaction. Yu *et al.* [14] also studied the magnetoresistance property of pseudo-spin-valve nanoscale elliptical rings with various aspect ratios. In this paper, we investigate the magnetization reversal behavior as functions of aspect ratios and thicknesses of single-layer elliptical ring arrays with external field parallel and perpendicular to the long axis.

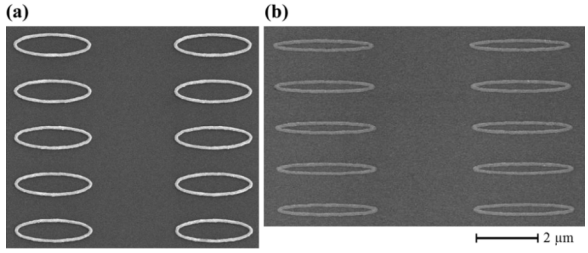

Fig. 1. SEM images of selected samples. (a) Aspect ratio $r = 3.3$. (b) $r = 8$ arrays of elliptical rings. The edge-to-edge distance in the long axis direction is fixed at 3 μm.

II. Experimental

Polycrystalline elliptical ring arrays were fabricated by electron-beam lithography techniques and lift-off process. We deposited NiFe films onto 50-nm SiO_2 coated silicon (100) substrates by dc magnetron sputtering. The base pressure of the sputter chamber was 5×10^{-7} Torr and working pressure was 1×10^{-3} Torr. The NiFe elliptical rings described here had fixed line width of 100 nm and circumference of 6.3 μm, various aspect ratios r (long axis to short axis) from 1.2 to 8, and thickness t ranging from 10 to 40 nm. Fig. 1 shows the scanning electron microscopy (SEM) images of (a) aspect ratio $r = 1.2$ and (b) $r = 8$ samples. For the magnetization reversal characteristics, we used a home-made longitudinal magnetooptical Kerr effect setup to detect magnetization component along the plane of incidence. The light source of 20-mW HeNe laser was polarized by a high extinction ratio Glan–Thompson prism to get s-wave polarization. The 5 μm diameter spot was focused with an objective lens. Reflective light passed through an achromatic lens and analyzer before entering the detector. Simulation of the magnetization configurations was made with

Manuscript received October 31, 2009; revised December 14, 2009; accepted January 04, 2010. Current version published May 19, 2010. Corresponding author: S.-F. Lee (e-mail: leesf@phys.sinica.edu.tw).

Color versions of one or more of the figures in this paper are available online at http://ieeexplore.ieee.org.

Digital Object Identifier 10.1109/TMAG.2010.2040593

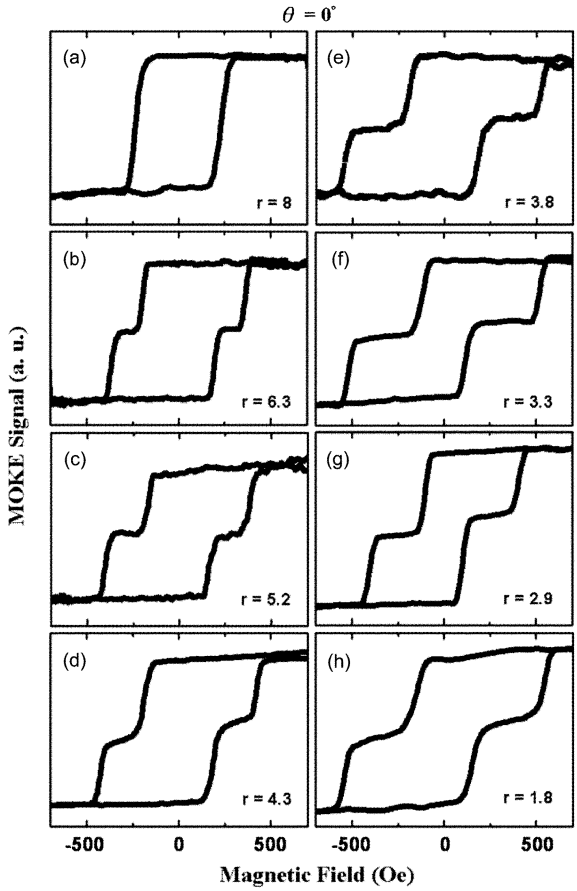

Fig. 2. (a)–(h) MOKE signals for 20-nm NiFe elliptical rings arrays of fixed width 100 nm and circumference 6.3 μm for applied field parallel to the long axis of varied aspect ratios.

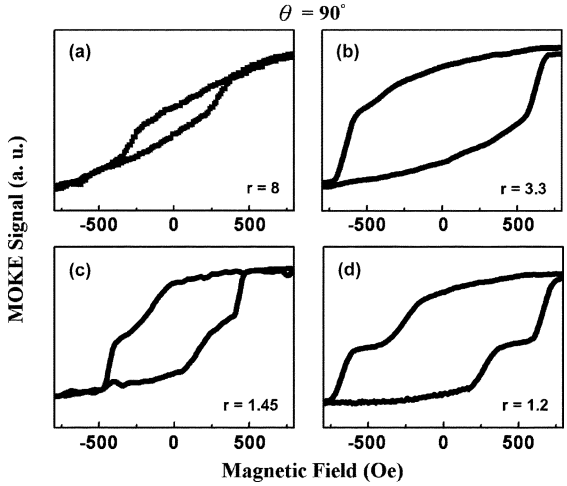

Fig. 3. MOKE signals for 20-nm NiFe elliptical rings arrays for applied field parallel to the short axis and varied aspect ratios from (a) $r = 8$ to (d) $r = 1.2$.

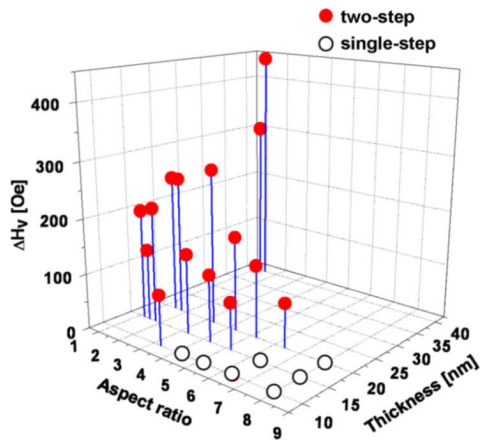

Fig. 4. Phase diagram of elliptical ring reversal behavior and the field range of the vortex state ΔH_v as functions of the aspect ratio r and thickness$t$ for the applied field parallel to the long axis. The solid and open circles represent two-step and single-step switching, respectively.

the OOMMF code [15]. Unit cell of a 5-nm cube and default values of material parameters for NiFe were used.

III. Results and Discussion

In Fig. 2(a)–(h), we present the hysteresis loops for 20-nm-thick NiFe elliptical ring arrays with different aspect ratios for the in-plane external field parallel $(\theta = 0°)$ and perpendicular $(\theta = 90°)$ to the long axis of the ring. From the MOKE signal, we observed that the transition between single-step and two-step switching depended sensitively on the ring structure and the field orientation. When the field was parallel to the long axis of the elliptical rings, except the ring with the $r = 8$, we found that the magnetization reversal processes occurred by two-step switching. As we have previously discussed [13], the two-step switching behavior indicated that the onion state obtained at high fields was energetically unfavorable at intermediate fields. Instead, formation of vortex state without domain walls was preferred. From Figs. 2(b)–(d), it can be seen that the range of flux closure plateau, ΔH_v, where vortex state exists, increased with decreasing aspect ratio. The ΔH_v increased from 95 Oe for the $r = 6.3$ to 180 Oe for the $r = 4.3$. It indicates that the stability of vortex state strongly depends on the aspect ratio of the elliptical ring. However, for the aspect ratio $r < 3.8$, as shown in Figs. 2(f)–(h), all the hysteresis loops display two-step switching with similar ΔH_v. The range of vortex stability $\Delta H_v = 250$ Oe to 310 Oe was found for the range of aspect ratio $1.8 \leq r \leq 3.8$. They represented that the similar spin reversal process behavior and the range of vortex state was independent of the variation of aspect ratio. It is noted that, for the $r = 3.3$, the field range of vortex state has a maximum value of 310 Oe.

When the field was applied along the short axis, as shown in Fig. 3(a)–(d), the two-step reversal behavior was only found in rings with lower aspect ratios, and there was a narrow field range of stability for the vortex state. For the $r = 3.3$ and $r = 8$, the hysteresis loops display the single switching process. For the $r = 1.45$ and $r = 1.2$, the distinct two-step switching was observed. The vortex state is unfavorable for the applied field perpendicular to the long axis of elliptical ring. This can be ascribed to the effect of demagnetization energy due to shape anisotropy and the higher Zeeman energy for movement of one of the domain walls to move across the elliptical ring to form the vortex state [8].

For the field along the long axis, Fig. 4 shows a phase diagram of elliptical ring reversal behavior and the field range of the vortex state ΔH_v as functions of the aspect ratio r and thickness t. The solid and open circles represent two-step and single-step switching, respectively. According to the hysteresis loops of our

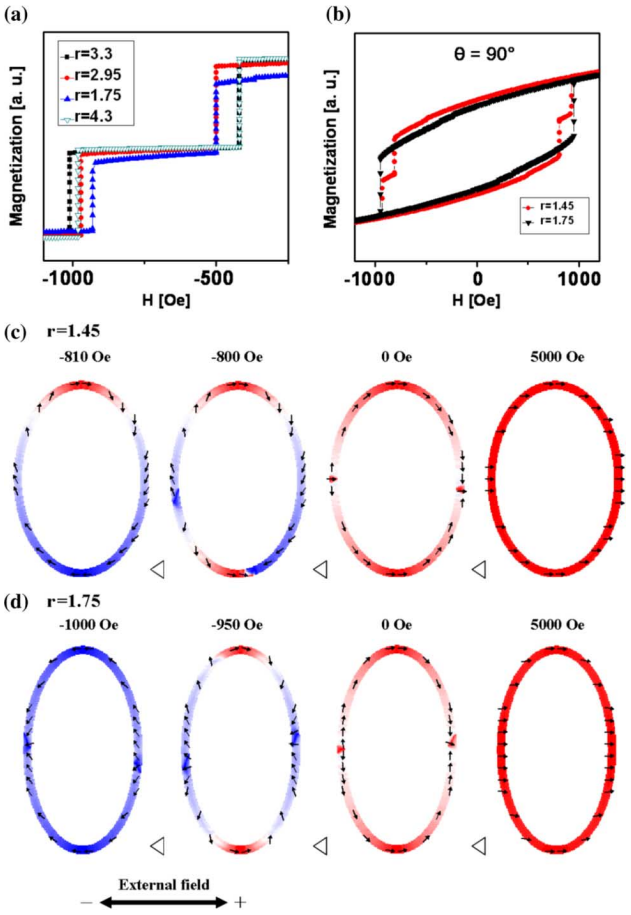

Fig. 5. Simulation loops for fields along the (a) long axis and (b) short axis of the 20-nm elliptical rings and varied aspect ratio. (c) and (d) Spin configurations with a single 20-nm NiFe ring of different aspect ratios for field applied along the short axis.

micro-MOKE experiment, we observed that the two-step reversals were present in the thicker rings or lower aspect ratios. At the same time, the width of the plateau for stable vortex states increased distinctly upon increasing the film thickness. When the aspect ratio decreased, however, the plateau width increased and then started to decrease, as can be seen in Fig. 2, for example. The largest width of the plateau occurred between $r = 1.5$ to 3.3 in the thicknesses we investigated.

Micromagnetic simulations of the magnetization orientation and the energy variations of the elliptical rings with respect to external fields were also investigated. The switching behavior agreed qualitatively with our experimental results. However, there is no quantitative agreement for the saturation fields and the range of vortex stability etc. This can be attributed to that there are thermal fluctuation and impurity effects in the experiments. Fig. 5(a) and (b) shows the simulation loops, and Fig. 5(c) and (d) shows the spin configurations with a single 20-nm NiFe ring of different aspect ratios for field applied along the short axis. When the field was along the long axis, the magnetization transition was through propagation of one of the transverse walls along one of the ring arcs and annihilated with the other wall, similar to the results shown in Fig. 5(c). The aspect ratio $r = 3.3$ sample has the largest plateau of stable vortex state as can be seen in Fig. 5(a). We show only one side of the loops because they are symmetrical. It showed the same behavior between the simulation and the experimental results. When the field was applied parallel to the short axis, as shown in Fig. 5(b), the hysteresis loops display single-step and two-step switching processes with $r = 1.75$ and $r = 1.45$, respectively. For the $r = 1.75$ [see Fig. 5(d)], the magnetization reversal was via coherent rotation. The transverse walls were pinned in the sides of the elliptical ring. During the onion state to reverse onion state transition, spin reversal occurred along the arcs of the long axis direction perpendicular to the external field. For the $r = 1.45$, shown in Fig. 5(c), the vortex state was present during the reversal process; the switching behavior of spin configuration was similar to the circular ring shape.

IV. Summary

In summary, the magnetization reversal characteristics in NiFe elliptical ring arrays have been investigated. When the field was parallel to the long axis, we showed that the phase diagram of elliptical ring reversal behavior and the field range of the vortex state ΔH_v are functions of the aspect ratio r and thickness t. We observed that the two-step reversals were present in the thicker rings or lower aspect ratios. Upon increasing the film thickness, the width of plateau for stable vortex state increased distinctly. With respect to the aspect ratio, the largest width of plateau was between 1.5 and 3.3 for the thickness between 10–40 nm we investigated. However, if the applied field was along the short axis, the two-step reversal behavior was only found in rings with lower aspect ratios, and there was a narrow field range of stability for the vortex state. For the single-step switching, the magnetization reversal was via coherent rotation along the arc of the long axis. For the two-step switching, the switching behavior of spin configuration was similar to the circular ring shape.

Acknowledgment

This work was supported by the National Science Council and the Academia Sinica of Taiwan.

References

[1] M. M. Miller, G. A. Prinz, S.-F. Cheng, and S. Bounnak, *Appl. Phys. Lett.*, vol. 81, p. 2211, 2002.
[2] J. G. Zhu, Y. Zheng, and G. A. Prinz, *J. Appl. Phys.*, vol. 87, p. 6668, 2000.
[3] M. Kläui, C. A. F. Vaz, L. J. Heyderman, U. Rüdiger, and J. A. C. Bland, *J. Magn. Magn. Mater*, vol. 290, p. 61, 2005.
[4] M. Kläui, C. A. F. Vaz, J. Rothman, J. A. C. Bland, W. Wernsdorfer, G. Faini, and E. Cambril, *Phys. Rev. Lett.*, vol. 90, p. 097202, 2003.
[5] S. Jain and A. O. Adeyeye, *Appl. Phys. Lett.*, vol. 92, p. 202506, 2008.
[6] Y. G. Yoo, M. Klaui, C. A. F. Vaz, L. J. Heyderman, and J. A. C. Bland, *Appl. Phys. Lett.*, vol. 82, p. 2470, 2003.
[7] J. Rothman, M. Klaui, L. Lopez-Diaz, C. A. F. Vaz, A. Bleloch, J. A. C. Bland, Z. Cui, and R. Speaks, *Phys. Rev. Lett.*, vol. 86, p. 1098, 2001.
[8] W. Jung, F. J. Castaño, and C. A. Ross, *Phys. Rev. Lett.*, vol. 97, p. 247209, 2006.
[9] C. A. Ross, F. J. Castaño, W. Jung, B. G. Ng, I. A. Colin, and D. Morecroft, *J. Phys. D: Appl. Phys.*, vol. 41, p. 113002, 2008.
[10] S. Jain and A. O. Adeyeye, *J. Appl. Phys.*, vol. 105, p. 07E904, 2009.
[11] F. J. Castaño, C. A. Ross, and A. Eilez, *J. Phys. D: Appl. Phys.*, vol. 36, p. 2031, 2003.
[12] Y. Ren and A. O. Adeyeye, *J. Appl. Phys.*, vol. 105, p. 063901, 2009.
[13] L. J. Chang, C. Yu, T. W. Chiang, K. W. Cheng, W. T. Chiu, S. F. Lee, Y. Liou, and Y. D. Yao, *J. Appl. Phys.*, vol. 103, p. 07C514, 2008.
[14] C. Yu, T. W. Chiang, Y. S. Chen, K. W. Cheng, D. C. Chen, S. F. Lee, Y. Liou, J. H. Hsu, and Y. D. Yao, *Appl. Phys. Lett.*, vol. 94, p. 233103, 2009.
[15] A three-dimensional code to calculate the magnetization configuration and its field evolution is described on http://math.nist.gov/oommf.